Time-dependent biological effects after ultraviolet light and nonthermal atmospheric pressure plasma treatment on aged titanium surface

Sung-Hwan Choi

Department of Dentistry

The Graduate School

Yonsei University

Time-dependent biological effects after ultraviolet light and nonthermal atmospheric pressure plasma treatment on aged titanium surface

A Dissertation

Submitted to the Department of Dentistry

and the Graduate School of Yonsei University

in partial fulfillment of the

requirements for the degree of

Doctor of Philosophy

Sung-Hwan Choi

December 2016

연세대학교
YONSEI UNIVERSITY

This certifies that the Dissertation of

Sung-Hwan Choi is approved.

Supervisor: Chung-Ju Hwang

Hyung-Seog Yu

Jung-Yul Cha

Jae-Hoon Lee

Kwang-Mahn Kim

The Graduate School

Yonsei University

December 2016

감사의 글

지금 이 순간 이 글을 쓸 수 있는 은혜를 베풀어 주신 주님께 감사 드립니다. 본 실험 논문이 완성되기까지 할 수 있다는 용기를 북돋아 주시고, 학업에 정진할 수 있도록 지도를 베풀어주신 황충주 교수님께 감사와 존경을 드립니다. 보다 좋은 논문을 위해 바쁘신 와중에도 귀중한 시간을 내어주시고, 필요한 순간 세심하고 소중한 조언을 아끼지 않으셨던 유형석 교수님, 차정열 교수님, 이재훈 교수님, 김광만 교수님께 진심으로 감사 드립니다. 부족한 제게 교정학을 배울 수 있는 기회를 주시고, 수련기간부터 지금까지 가르침으로 이끌어 주신 박영철 명예교수님, 백형선 교수님, 김경호 교수님, 이기준 교수님, 정주령 교수님, 최윤정 교수님께 감사 드립니다.

논문 투고 시 소중한 조언을 아끼지 않으셨던 최은하 교수님께 감사 드립니다. 실험을 위해 많은 도움을 주었던 정원석 선생, 권재성 선생, 김도현 선생에게 감사의 말씀을 드립니다. 그리고 저를 낳아주시고 사랑으로 길러주신 부모님, 저를 믿고 응원해 주신 장인어른과 장모님, 그리고 사랑하는 아내 강다영과 소중한 딸 수현이와 함께 이 기쁨을 함께 나누고 싶습니다.

2016 년 12 월

저자 씀

Table of Contents

List of Figures

Abstract

Time-dependent biological effects after ultraviolet light and nonthermal atmospheric pressure plasma treatment on aged titanium surface

Sung-Hwan Choi

Department of Dentisry

The Graduate School, Yonsei University

Ultraviolet light (UV) or nonthermal atmospheric pressure plasma jet (NTAPPJ) treatment has been known to modify the physicochemical properties of titanium implants without altering topography and to enhance its biological activity, such as promoting blood protein and osteoblastic cell attachment, thereby increasing the formation of new bone. However, few studies have evaluated whether there are differences in time-dependent biological activity of treatment on the titanium surface between UV and

NTAPPJ. Therefore, we evaluated time-dependent biological effects after UV and NTAPPJ treatment on aged titanium surface compared with that of untreated titanium surface.

Grade IV machined surface titanium discs (12-mm diameter) were used immediately and stored up to 28 days after UV irradiation for 15 minutes or NTAPPJ treatment for 10 minutes. Changes of surface characteristics over time were evaluated using scanning electron microscopy, surface profiling, contact angle analysis, X-ray photoelectron spectroscopy, and surface zeta-potential. Changes in biological activity over time were as determined by analyzing bovine serum albumin adsorption, MC3T3-E1 early adhesion and morphometry, and alkaline phosphatase (ALP) activity between groups.

We found no differences in the effects of treatment on titanium between UV and NTAPPJ regardless of the storage time ($P > 0.05$). Photocatalytic activity by UV and higher production of reactive oxygen species (ROS) such as hydroxyl radical or synergistic ROS/UV action by NTAPPJ removed the surface hydrocarbon and altered the surface from negatively charged hydrophobic (bioinert) to positively charged hydrophilic (bioactive) surfaces ($P < 0.001$). These effects immediately after UV and NTAPPJ treatment enhanced albumin adsorption ($P < 0.001$), early osteoblastic cell attachment ($P < 0.05$), and cytoskeleton development ($P < 0.001$). 28 days after UV or NTAPPJ treatment, there were no differences in cell adhesion and cytoskeleton development between groups ($P > 0.05$). However, ALP activity of the UV- and NTAPPJ-treated

groups was significantly increased when compared with that of the untreated titanium ($P < 0.05$).

Based on the results of this study, there was no significant difference in the biological effect of treatment on the titanium surface between UV and NTAPPJ over time. When compared to immediately after treatment, these treatment effects decreased with time. However, UV and NTAPPJ treatment can enhance the biological activity of aged titanium surface compared with that of untreated titanium regardless of the storage time. Future *in vivo* studies are necessary to confirm whether these results can be applied in real clinical situations in the medical and dental fields.

Key words: Titanium; Implant; Ultraviolet; Nonthermal atmospheric pressure plasma jet; Hydrophilicity; Hydrocarbon; Photocatalytic activity; Reactive oxygen species; Biological activity

Time-dependent biological effects after ultraviolet light and nonthermal atmospheric pressure plasma treatment on aged titanium surface

Sung-Hwan Choi

Department of Dentisry

The Graduate School, Yonsei University

(Directed by Professor Chung-Ju Hwang, D.D.S, M.S, Ph.D)

I. INTRODUCTION

Titanium is commonly used in prosthetic implants for restoring joint function and relieving pain in joint arthroplastic operation, in dental implants for rehabilitation of missing teeth, and as an absolute skeletal anchorage, because the oxidised titanium surface exhibits excellent biological compatibility and can achieve tight mutual contact with adjacent bone without formation of fibrous tissue surrounding the implants, a feature called osseointegration (Albrektsson and Johansson, 2001). Nevertheless, the rate of

revision surgery for orthopaedic joint implants is over 10% within 15 years of the initial surgery, primarily owing to aseptic loosening through lack of sufficient bone-implant integration without concurrent trauma or infection (Drees et al., 2007; Fender et al., 2000). Five-year success rates for titanium dental implants range from 90.1% to 96.5% for the fixed prosthesis type; however, the success rates decrease over time, reaching 89% and 83% after 10 and 16 years, respectively (Simonis et al., 2010). Patients at higher risk, i.e. those with bone compromised by systemic diseases such as diabetes, aging, poor bone quality (D3-D4) or previous periodontal disease, exhibit higher long-term failure rates (Dalago et al., 2016; Fransson et al., 2008; Misch et al., 1999). Such implant failure can lead to increased patient dissatisfaction and high socioeconomic burden, particularly in older patients.

In order to prevent or reduce the possibility of implant failure, various topographical modifications to the titanium surface, such as sand-blasted, large grit, acid etched (SLA) or anodic oxidation, have been used to increase surface roughness and thereby improve surrounding osteoblastic cell adhesion, proliferation, and differentiation (Choi et al., 2016; Le Guehennec et al., 2007; Rani et al., 2012; Wennerberg et al., 2013). However, previous studies have reported that these surface modifications are limited to activation of the bioinert titanium surface because the bioactivity and osteoconductivity of the titanium surface decrease over time and because commercially available titanium devices are sold as sufficiently aged with packaging, regardless of the type of surface treatment (Aita et al., 2009; Att et al., 2009; Iwasa et al., 2011).

Previous studies reported that time-dependent degradation of the bioactivity of titanium surface caused the decrease in the biomechanical strength of bone-titanium integration compared with newly prepared titanium surface at the early healing stage in an animal model (Att et al., 2009; Lee and Ogawa, 2012). This biological degradation of titanium surface was associated with considerably reduced capability of aged titanium surfaces to protein and osteogenic cell adhesions due to progressive accumulation of hydrocarbon on the titanium surface (Att et al., 2009; Lee and Ogawa, 2012).

Recently, ultraviolet light (UV) or nonthermal atmospheric pressure plasma jet (NTAPPJ) treatment has been shown to modify the physicochemical properties of titanium and to enhance its biologic capability without altering topography (Aita et al., 2009; Hirakawa et al., 2013; Minamikawa et al., 2014; Pyo et al., 2013; Seo et al., 2014; Seo et al., 2015). These treatments can change the titanium surface from hydrophobic to hydrophilic due to removal of surface hydrocarbon and/or formation of chemically reactive hydroxyl radical species with reduced surface negative charge (Attri et al., 2015; Wang et al., 1997; Wu et al., 2015). Moreover, Bacakova et al. reported that cell adhesion was promoted by a moderately hydrophilic and less negatively charged surface (Bacakova et al., 2011). However, most previous studies have only investigated cellular responses immediately after treatment by each method. For example, Canullo et al. reported that the beneficial effects of various titanium implanted surfaces immediately after argon plasma treatment for 12 min were comparable to those immediately after UV treatment for 3 h *in vitro* (Canullo et al., 2016). Based on the potential for clinical

application, the study included considerably different irradiation times for the two methods, although the UV irradiation time could probably be shortened using higher UV flux lamps. Additionally, the study focused only on the immediate effects of treatment on the cellular response.

To the best our knowledge, few studies have evaluated the effects of treatment on the titanium surface between UV and NTAPPJ or time-dependent aging of the titanium surface after UV or NTAPPJ treatment. Each method has been successfully applied with increased bone-implant contact *in vivo*, and no significant intergroup differences in histological inflammatory reactions by the recipient's immune system have been identified (Giro et al., 2013; Hayashi et al., 2014; Pyo et al., 2013; Shen et al., 2016; Teixeira et al., 2012). However, in order to ensure the validity of UV or NTAPPJ treatment before clinical application, it is necessary to confirm that treatment effects are maintained for at least up to 4–8 weeks, during the early healing time for bone formation after implantation (Degidi et al., 2009; Gapski et al., 2003).

Therefore, in this study, we aimed to evaluate time-dependent biological effects after UV and NTAPPJ treatment on aged titanium surface compared with that of untreated titanium surface.

II. MATERIALS AND METHODS

1. Preparation of titanium samples

Titanium samples were prepared in a disc shape (12.0 mm in diameter, 1.0 mm thickness) by machining commercially of pure titanium (grade IV; Osstem Implant Co., Seoul, Korea). The titanium discs were sequentially cleaned with acetone, alcohol, and distilled water for 15 min each using an ultrasonic cleaner and then sterilised using ethylene oxide (EO) gas at a temperature of 55 °C for 1 h (Seo et al., 2014; Uhm et al., 2014).

The prepared titanium discs were stored in sealed 12-well cell culture plates under dark ambient conditions at room temperature over 8 weeks for a full aging (Iwasa et al., 2011; Minamikawa et al., 2014). After the storage, some titanium discs were treated by UV or NTAPPJ for a similar time.

UV irradiation was carried out for 15 min using a photo device (TheraBeam Affiny; Ushio Inc., Tokyo, Japan; Figure 1). The UV was delivered as a mixture of spectra via a UV lamp, and the measured intensities were 0.05 mW/cm^2 (λ = 360 ± 20 nm) and 2 mW/cm^2 (λ = 250 ± 20 nm)(Tuna et al., 2015). The distance between the disc and the UV lamp was fixed.

NTAPPJ treatment was performed with a compressed air gas flow of 5000 sccm (standard cubic centimetre per minute) for 10 min using a device at the Plasma Bioscience Research Center (Kwangwoon University, Seoul, Korea; Figure 2A-B)(Hong et al., 2009; Seo et al., 2014). Briefly, the distance between the plasma jet tip and the

titanium sample surface was set to 3 mm, and the maximum voltage was set to 17 kV. This NTAPPJ device consisted of a stainless steel inner electrode with 1.2 mm depth and 0.2 mm thickness along with quartz (3.2 mm depth) as the dielectric. These UV- or NTAPPJ-treated titanium discs were used immediately for each experiment or stored under dark ambient conditions for 3, 7, 14, or 28 days before starting each experiment. The control group was defined as sufficiently aged titanium discs without any treatment.

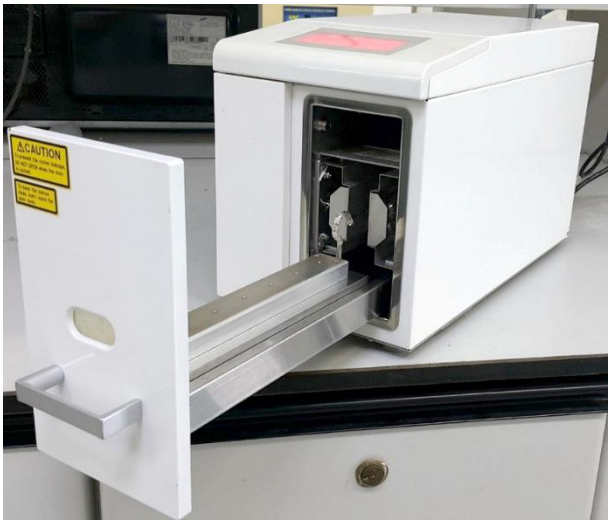

Figure 1. A photo device (TheraBeam Affiny; Ushio Inc., Tokyo, Japan) for ultraviolet light (UV) irradiation. The UV was delivered as a mixture of spectra via a UV lamp, and the measured intensities were 0.05 mW/cm^2 (λ = 360 ± 20 nm) and 2 mW/cm^2 (λ = 250 ± 20 nm).

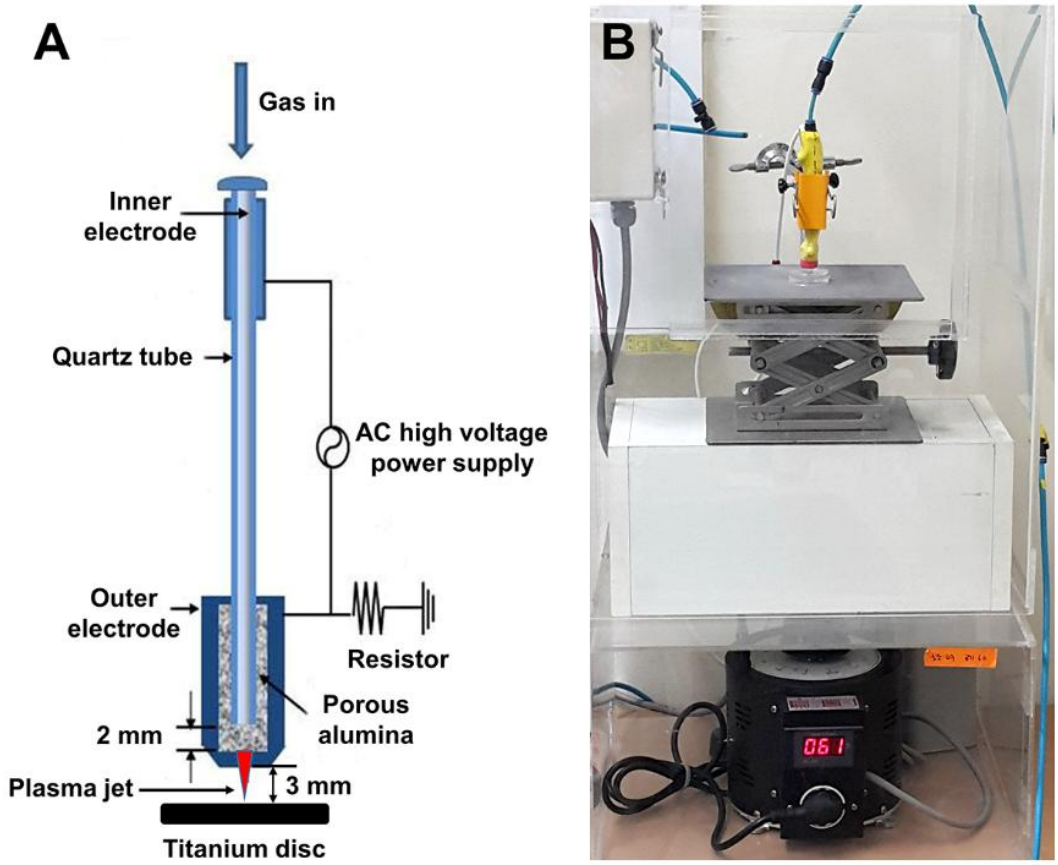

Figure 2. A nonthermal atmospheric pressure plasma jet (NTAPPJ) device manufacture by the Plasma Bioscience Research Center (Kwangwoon University, Seoul, Korea). Schematic diagram (A) and the actual photograph (B) of NTAPPJ. The distance between the plasma jet tip and the titanium sample surface was set to 3 mm, and the maximum voltage was set to 17 kV. This NTAPPJ device consisted of a stainless steel inner electrode with 1.2 mm depth and 0.2 mm thickness along with quartz (3.2 mm depth) as the dielectric.

2. Surface characterization

The surface morphologies of the samples were examined immediately after treatment by UV or NTAPPJ and for the untreated control group using scanning electron microscopy (SEM; Hitachi S3000N; Hitachi, Tokyo, Japan) and an optical three-dimensional surface profiler (ContourGT; Bruker, AZ, USA; Figure 3) using the vertical scanning interferometry (VSI) mode with a green luminous source. Surface roughness parameters, including average roughness (Sa) and peak-to-valley roughness (Sz) values, were measured at a magnification of 10× with a scanning area of 310 μm × 230 μm.

Figure 3. An optical three-dimensional surface profiler (ContourGT; Bruker, AZ, USA).

Changes in the hydrophilicity of the titanium disc surface after treatment over time were assessed by measuring the contact angle and spread area of a 4-μL H_2O droplet on the centre of each sample surface. Ten seconds after the drop fell on the surface, the data were captured using a video contact angle goniometer (Phoenix 300; SEO, Gyeonggi-do, Korea; Figure 4) to calculate the contact angle and spread area using Image XP software (SEO) immediately or at 3, 7, 14, or 28 days after UV or NTAPPJ treatment.

The chemical composition of the titanium disc surface immediately and 28 days after treatment using UV or NTAPPJ was evaluated using X-ray photoelectron spectroscopy (XPS; K-alpha; Thermo VG, UK), operated using a monochromatic Al Kα line (1486.6 eV) with the following parameters: 12 kV, 3 mA, and a spot size of 400 μm. The titanium, oxygen, and carbon contents were examined under vacuum conditions at each time point.

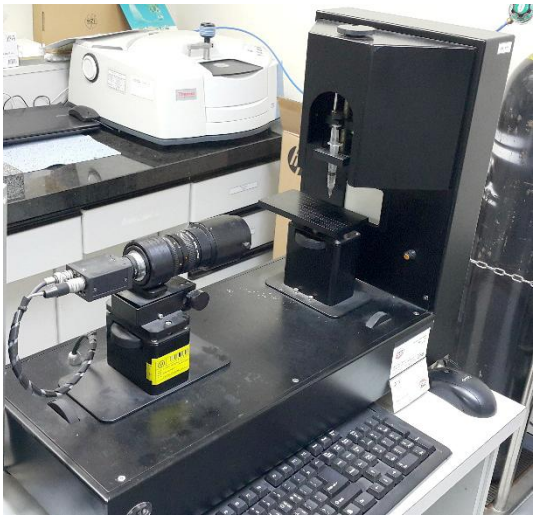

Figure 4. A video contact angle goniometer (Phoenix 300; SEO, Gyeonggi-do, Korea).

3. Zeta potential

To investigate changes in the zeta potential of the titanium disc surface immediately and 28 days after treatment using UV or NTAPPJ, the samples were dispersed with monitor particles (polystyrene latex) in a high-purity silica glass cell. This glass cell was connected into a laser electrophoresis spectroscope (ELSZ 1000; Otsuka Electronics Co., Osaka, Japan; Figure 5) to measure the zeta potential of the surface (Kim et al., 2003). The electrophoretic mobility or zeta potential is highly dependent on both the sample surface and the medium in which it is immersed. By measuring the zeta potential of monitor particles as a function of distance from the surface of investigation, the surface zeta potential can be obtained. The measurements were performed in 10 mM NaCl solution at pH 7.4. The data were selected when the distribution of zeta potential according to the height of the cuvette was parabolic from the centre. The electrokinetic streaming potential was automatically calculated using the Smoluchowski method.

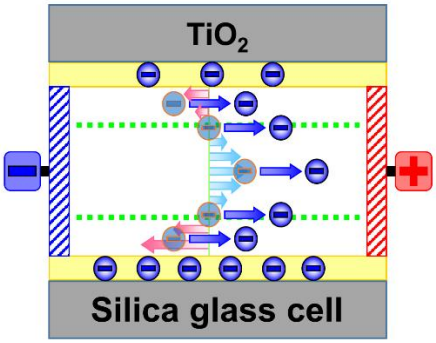

Figure 5. A schematic diagram for laser electrophoresis spectroscope, modified from the manufacturer's manual. The electrophoretic mobility of the monitor particles is highly dependent on the zeta potential of the titanium disc surface.

4. Protein adsorption assay

Bovine serum albumin, fraction V (BSA; Pierce Biotechnology, Inc., IL, USA) was used as a model protein. The protein solution (100 μL; 1 mg/mL in phosphate-buffered saline [PBS], pH 7.4) was pipetted onto and spread over each sample surface immediately and 28 days after treatment using UV or NTAPPJ treatment. After 4 h of incubation under sterile humidified conditions at 37 °C in 5% CO_2, nonadherent protein removed by washing with PBS two times. Amounts of protein were measured by 200 μL microbicinchoninic acid (MicroBCA) based on total protein assay kit (Pierce Biotechnology, Inc., IL, USA) followed by incubation at 37 °C for 30 min (Aita et al., 2009; Att et al., 2009). The optical density (OD) of each sample was quantified using a microplate reader (Epoch, BioTek Instruments, VT, USA; Figure 6) at 562 nm, and the rate of protein adsorption was calculated as the percentage of albumin adsorbed to the sample surface relative to the total amount using a BSA standard curve provided with the kit.

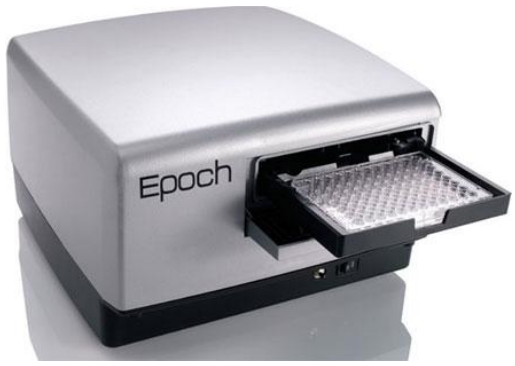

Figure 6. A microplate reader (Epoch, BioTek Instruments, VT, USA), from the manufacturer's homepage.

5. Cell culture

Murine MC3T3-E1 osteoblast cells (CRL-2593; American Type Culture Collection, VA, USA) were used at passages 7–9, regardless of storage time, to determine the cellular responses to the treatments. The cells were cultured in alpha-MEM cell culture medium (Gibco, NY, USA) containing 10% fetal bovine serum (FBS; Gibco), penicillin (100 U/mL; Gibco), and streptomycin (100 mg/mL; Gibco) at 37 ℃ in 5% CO_2. After reaching 80% confluence, the cells were detached using 0.25% trypsin/1 mM EDTA-4Na (Gibco) to prevent contact inhibition. The cell culture medium was changed every 48 h.

6. Cell adhesion assay

A total of 1×10^4 cells in 100 μL was placed onto each sample surface in a 24-well plate immediately and 28 days after treatment with UV or NTAPPJ. After 4 or 24 h of incubation, these quantifications were performed using water-soluble tetrazolium salt (WST)-based colorimetry (EZ-1000; DoGenBio Co., Gyeonggi-do, Korea). The cells were incubated at 37 ℃ for 4 h with tetrazolium salt (WST) reagent, and the amount of formazan product was measured using a microplate reader (Epoch; BioTek Instruments) at 450 nm. The results were expressed as the relative percentage of cells attached to the sample surface compared with that of the control group.

7. Cell morphology and morphometry

A total of 1 × 10^4 cells in 100 μL was placed onto each sample surface in a 24-well plate immediately and 28 days after treatment with UV or NTAPPJ. After incubation of cells on treated or untreated titanium disc surfaces for 4 h at 37 °C in 5% CO_2, cells were stained using diamidino-2-phenylindole, dihydrochloride (DAPI; blue for nuclei; Molecular Probes, Invitrogen, NY, USA) and rhodamine phalloidin (red for F-actin filaments; Molecular Probes). Confocal laser-scanning microscopy (LSM 700; Carl Zeiss, Jena, Germany; Figure 7A) was used to examine cell morphology and cytoskeletal arrangement. Twelve single cells with typical morphology feature were randomly selected from three different points on the titanium surface (Uchiyama et al., 2014). Quantitative assessment of cell area, perimeter, and Feret's diameter (Figure 7B) was performed using ImageJ software (NIH, Bethesda, MD, USA).

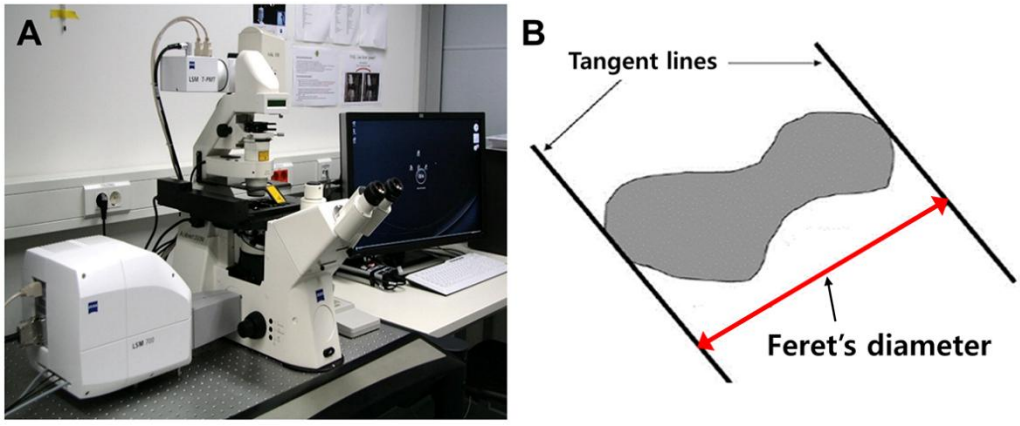

Figure 7. (A) A confocal laser-scanning microscopy and (B) Feret's diameter. It can be defined as the distance between the two parallel planes restricting the object perpendicular to that direction.

8. Alkaline phosphatase (ALP) activity

A total of 1×10^4 cells in 100 μL was placed onto each sample surface in a 24-well plate immediately and 28 days after treatment with UV or NTAPPJ. After 7 days of incubation of cells on treated or untreated titanium discs, cells were lysed with 0.2% Triton X-100 (Sigma-Aldrich, Inc., MO, USA) (Iwasa et al., 2011). The lysates were then centrifuged, and the supernatants were reacted with *p*-nitrophenylphosphate (*p*NPP) substrate from an ALP assay kit (SensoLyte *p*NPP Alkaline Phosphatase Assay Kit; AnaSpec, CA, USA) at room temperature for 60 min. The optical density (OD) was read at 405 nm using a plate reader (Epoch; BioTek Instruments).

9. Statistical analysis

All statistical analyses were performed using IBM SPSS software, version 21.0 (IBM Korea Inc., Seoul, Korea) for Windows. According to previous studies (Canullo et al., 2016; Seo et al., 2014; Wu et al., 2015), at least four samples for each experiment were used, and each experiment was repeated three times. The results between three groups (the control, UV, and NTAPPJ) at each time point were analysed by one-way analysis of variance (ANOVA) with Tukey's method. Differences with *P* values of less than 0.05 were considered statistically significant.

III. RESULTS

1. Surface characterization

SEM analysis confirmed that the titanium discs used in this study showed typical lathe marks left by the milling process for machined titanium surfaces. The UV- or NTAPPJ-treated titanium discs showed no marked differences in surface roughness parameters, including Sa and Sz, as compared with the control group under three-dimensional surface analysis (Figure 8A–E). Sa values of the control, UV-treated, and NTAPPJ-treated groups were (0.32 ± 0.03) μm, (0.28 ± 0.05) μm, and (0.27 ± 0.03) μm, respectively ($P > 0.05$). Sz values of the control, UV-treated, and NTAPPJ-treated groups were (3.75 ± 0.15) μm, (3.60 ± 0.28) μm, and (3.58 ± 0.37) μm, respectively ($P > 0.05$).

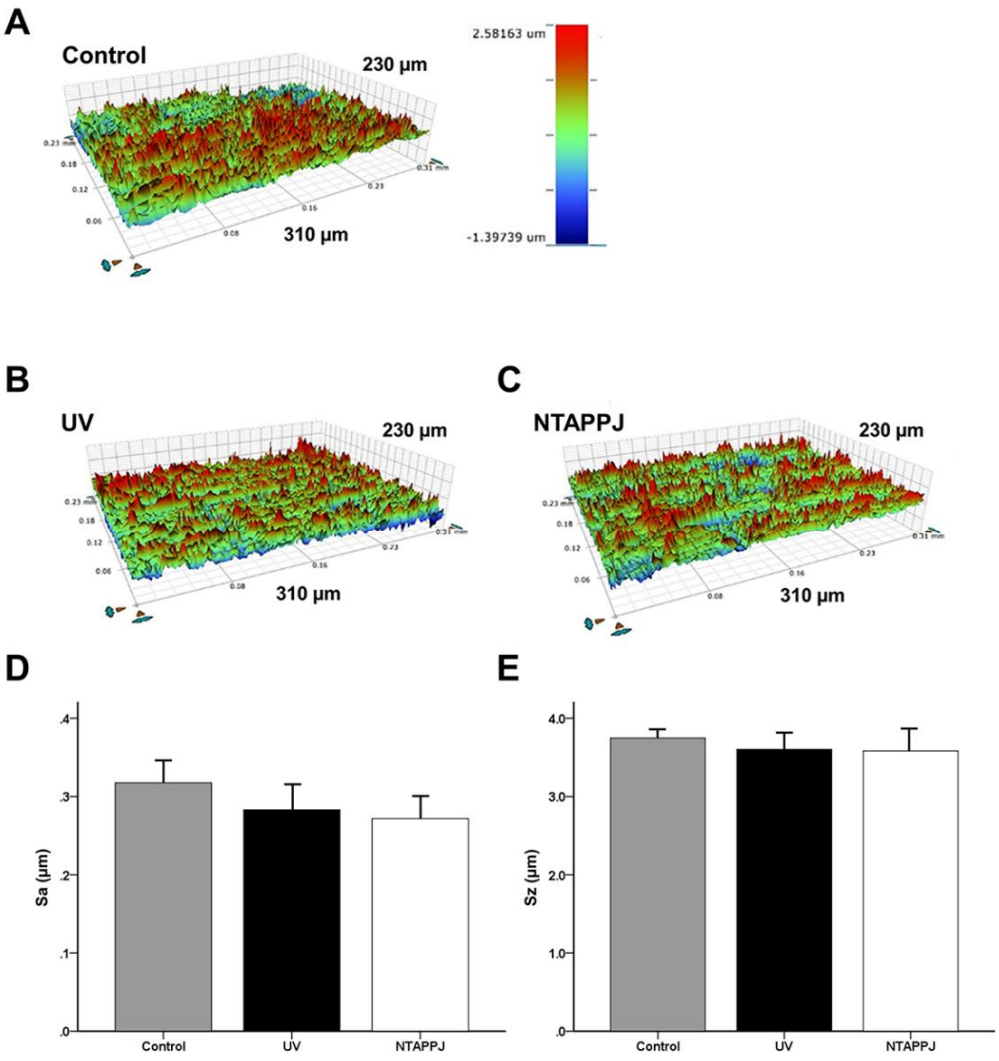

Figure 8. Surface morphology of the titanium discs. (A–C) Three-dimensional (3D) surface topographic images of the titanium disc surface immediately after UV and NTAPPJ compared with that of the control group. Surface roughness parameters, Sa (D) and Sz (E), were quantitatively measured at a magnification of 10× with a scanning area of 310 μm × 230 μm, and the results were compared between groups.

However, there was a significant difference in wettability by water between groups ($P < 0.001$; Figure 9A–G). As shown in Figure 9A, the H_2O droplet did not spread and maintained an arc shape on the titanium disc surface in the control group. The contact angle and spread area of the control group were (89.56 ± 3.97)° and (0.82 ± 0.04) mm^2, respectively. In contrast, in the UV- and NTAPPJ-treated groups, the contact angles and spread areas on the titanium surface were shifted from (15.50 ± 1.79)° to (49.08 ± 7.84)° and from (3.31 ± 0.39) mm^2 to (1.27 ± 0.17) mm^2, respectively, at 0 and 28 days after UV treatment, respectively. Similarly, the contact angles and spread areas on NTAPPJ-treated titanium discs were also shifted from (12.14 ± 3.14)° to (39.31 ± 2.36)° and from (3.36 ± 0.20) mm^2 to (1.50 ± 0.21) mm^2, respectively, over time. There were no significant differences in contact angles and spread areas between the UV- and NTAPPJ-treated groups, regardless of the storage time ($P > 0.05$).

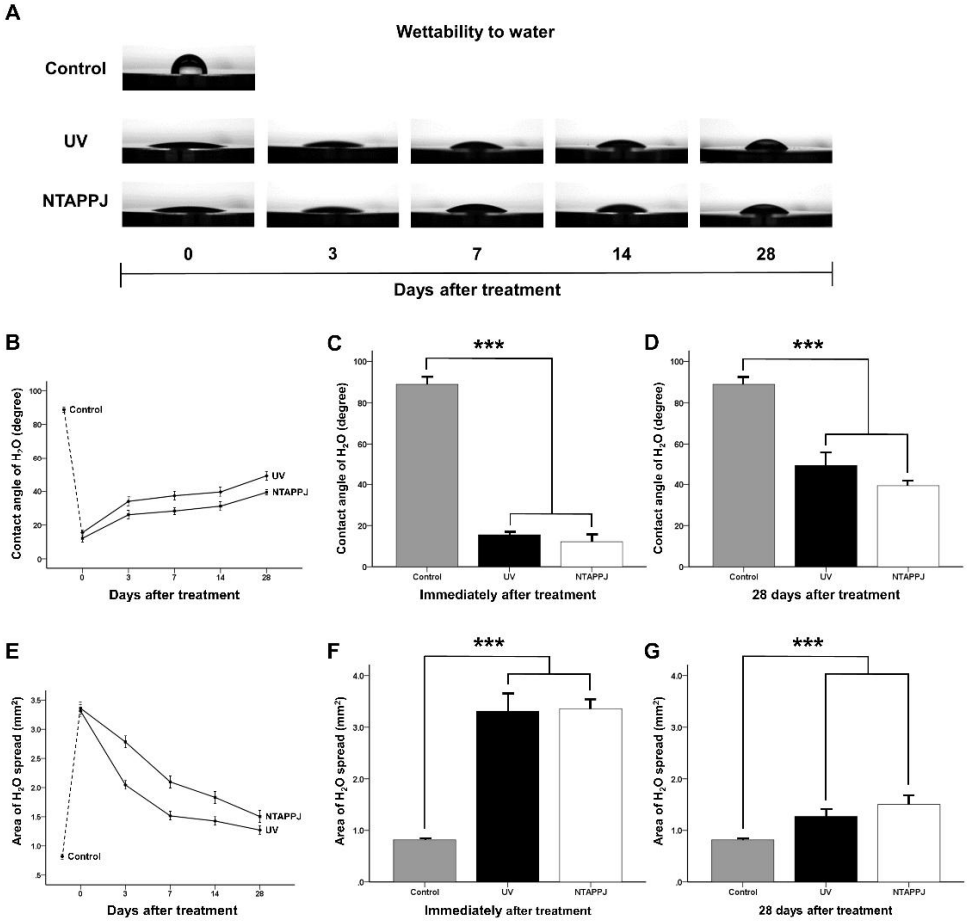

Figure 9. Changes in the hydrophilicity of the titanium disc surface after treatment over time. (A) Changes in wettability by water over time, as measured using a 4-μL H_2O droplet on the centre of each sample surface, between UV- and NTAPPJ-treated discs. (B) Changes in the contact angle with the titanium disc surface over time for the UV- and NTAPPJ-treated groups. Comparison of changes in the contact angle immediately (C) and 28 days (D) after treatment between groups. (E) Changes in the spread area of the titanium disc surface over time. Comparison of changes in the spread area immediately (F) and 28 days (G) after treatment between groups. ***$P < 0.001$ for comparisons between groups.

2. Changes in surface chemical compositions in the UV- and NTAPPJ-treated groups

As shown in Figure 10A, the peaks corresponding to the Ti2p 1/2 and Ti2p 3/2 components were located at binding energies from 458.7 to 464.3 eV, and the peaks in the experimental groups were higher than those in the control group, regardless of the storage time. The major peak corresponding to TiO_2 of the O1s spectra was located at a binding energy of 530.1 eV and was increased in the experimental groups compared with that in the control group, regardless of the storage time (Figure 10B). In particular, the peak corresponding to the hydroxyl group (-OH) at a binding energy of 532.0 eV for the NTAPPJ-treated titanium discs was increased compared with those of UV-treated and control titanium discs. However, the peaks of both UV- and NTAPPJ-treated groups were markedly decreased over time. In the C1s peaks, the peak corresponding to the hydrocarbon (-CH) at a binding energy of 284.7 eV was decreased in the experimental groups compared with that in the control group (Figure 10C). Similarly, the atomic percentages of carbon in the UV- and NTAPPJ-treated groups were lower than those in the control group, regardless of the storage time. The carbon contents immediately after UV or NTAPPJ treatment were markedly shifted from 49.48% to 17.95% or 19.35%, respectively, at 28 days after treatment (Figure 10D).

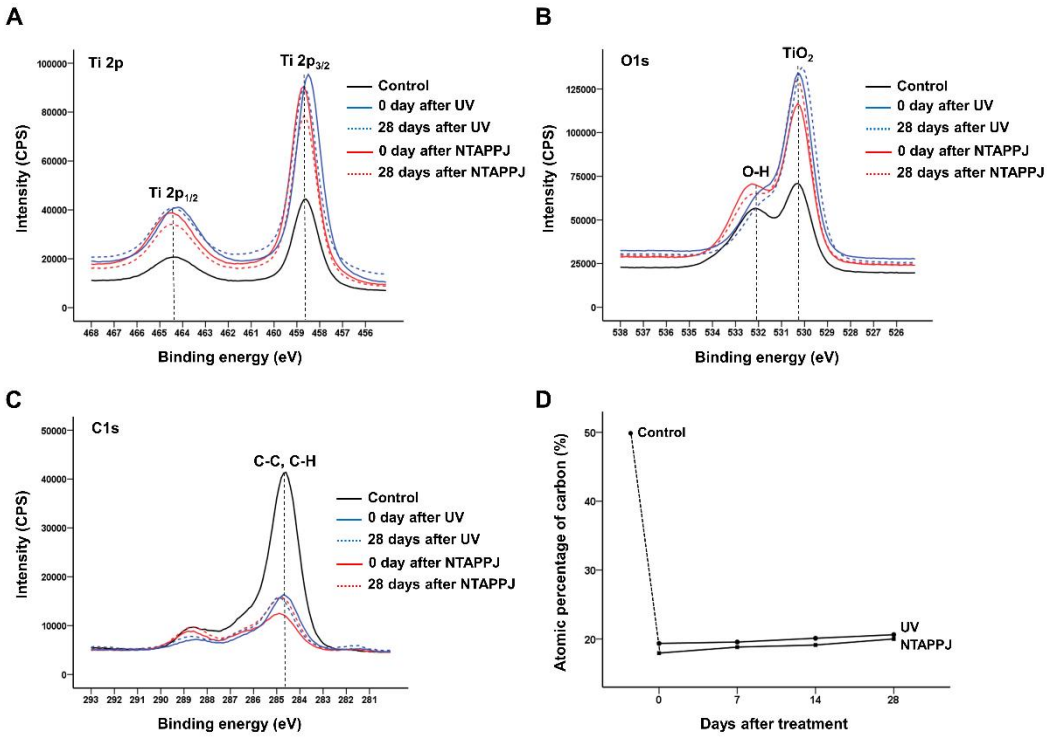

Figure 10. Changes in the chemical composition of the titanium disc surface after treatment over time. Changes in Ti2p (A), O1s (B), and C1s (C) spectra immediately and 28 days after treatment between groups. (D) Changes in atomic percentages of carbon over time after treatment between groups.

3. Decreased negative charges in UV- and NTAPPJ-treated groups

The zeta potential of the sample surface of the control group was highly negative (-9.59 ± 0.33) mV at pH 7.4 (Figure 11A–C). The zeta potentials increased immediately after UV or NTAPPJ treatment to (-2.99 ± 0.43) and (-2.58 ± 0.12) mV, respectively, and were significantly different compared with those of the control group ($P < 0.001$; Figure 11B). At 28 days after treatment, the zeta potentials of UV- and NTAPPJ-treated groups were markedly decreased to (-8.38 ± 0.17) and (-7.10 ± 0.53) mV, respectively, and were significantly different compared with those of the control group ($P = 0.001$; Figure 11C). There were no significant differences in the zeta potentials of the UV- and NTAPPJ-treated groups, regardless of the storage time ($P > 0.05$).

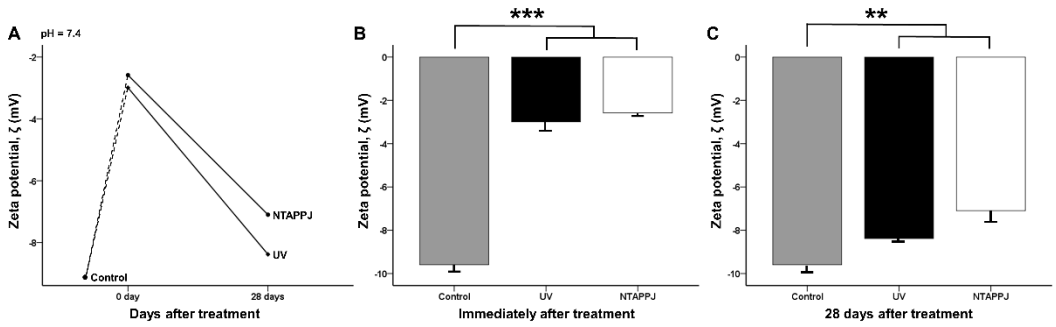

Figure 11. (A) Changes in the zeta potential of the titanium disc surface after treatment over time at pH 7.4. Comparison of changes in zeta potential immediately (B) and 28 days (C) after treatment between groups. **$P < 0.01$, ***$P < 0.001$ for comparisons between groups.

4. Protein adhesion capacity in the UV- and NTAPPJ-treated groups

Immediately after UV or NTAPPJ treatment, the amounts of BSA adsorbed to the titanium surface during the 4-h experimental period were significantly greater than those of the control group ($P < 0.001$; Figure 12A).

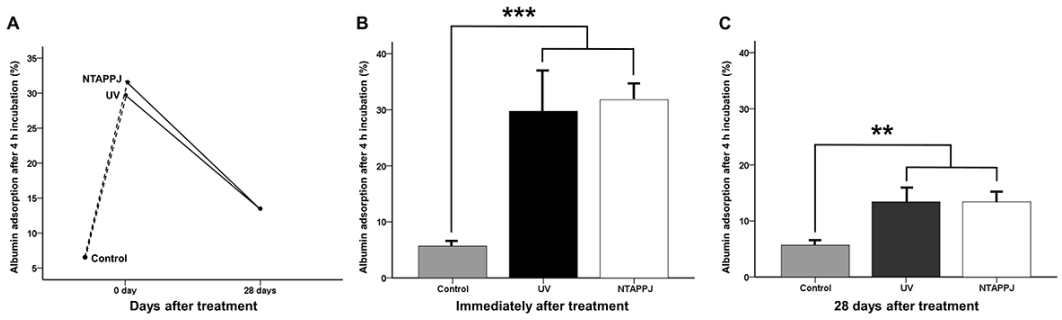

Figure 12. (A) Changes in albumin adsorption rates on the titanium disc surface after treatment over time. Comparison of changes in albumin adsorption rates immediately (B) and 28 days (C) after treatment between groups. $^{**}P < 0.01$, $^{***}P < 0.001$ for comparisons between groups.

The rate of BSA adsorption to the titanium discs relative to the total protein in the control group was 5.68% ± 1.06%. In UV- and NTAPPJ-treated groups immediately after treatment, the rates of BSA adhesion to the titanium discs increased to 29.73% ± 8.64% and 31.78% ± 2.72%, respectively (Figure 12B). These rates decreased to about 13.4% (UV, 13.40% ± 3.06%; NTAPPJ, 13.40% ± 1.89%) at 28 days after treatment. Although

these rates were not different between experimental groups, significant differences were observed compared with the control group, indicating that the electrical polarity of the 28-day-old treated titanium disc surface was sufficient for induction of albumin adhesion to the titanium surface compared with that of the control group ($P = 0.004$; Figure 12C).

5. Cellular adhesion capacity in UV- and NTAPPJ-treated groups

After 4 or 24 h of incubation, the number of adherent cells was increased for UV- and NTAPPJ-treated samples used immediately after treatment as compared with that of the control group (Figure 13A, B). The greater number of attached cells was observed on the titanium disc surface immediately after treatment using UV or NTAPPJ compared with that of the control group and 28-day-old treated titanium discs (Figure 14A). When the cellular attachment ratio of the control group was set at 100%, the relative cellular attachment ratios on UV- or NTAPPJ-treated surfaces were significantly increased to about 119% (UV, 119.69% ± 8.87%; NTAPPJ, 119.18% ± 3.39%) after incubation for 4 h (P = 0.002; Figure 10A) and about 117% (UV, 116.86% ± 10.68%; NTAPPJ, 117.27% ± 7.88%) after incubation for 24 h (P = 0.049; Figure 13B) as compared with that in the control group. However, 28 days after treatment, there were no significant differences in cellular attachment between groups, regardless of the incubation time, indicating that the 28-day-old treated titanium disc surface was not able to promote osteoblastic cell adhesion to the titanium disc surface, regardless of the type of treatment (Figures 13C, 13D, and 14A).

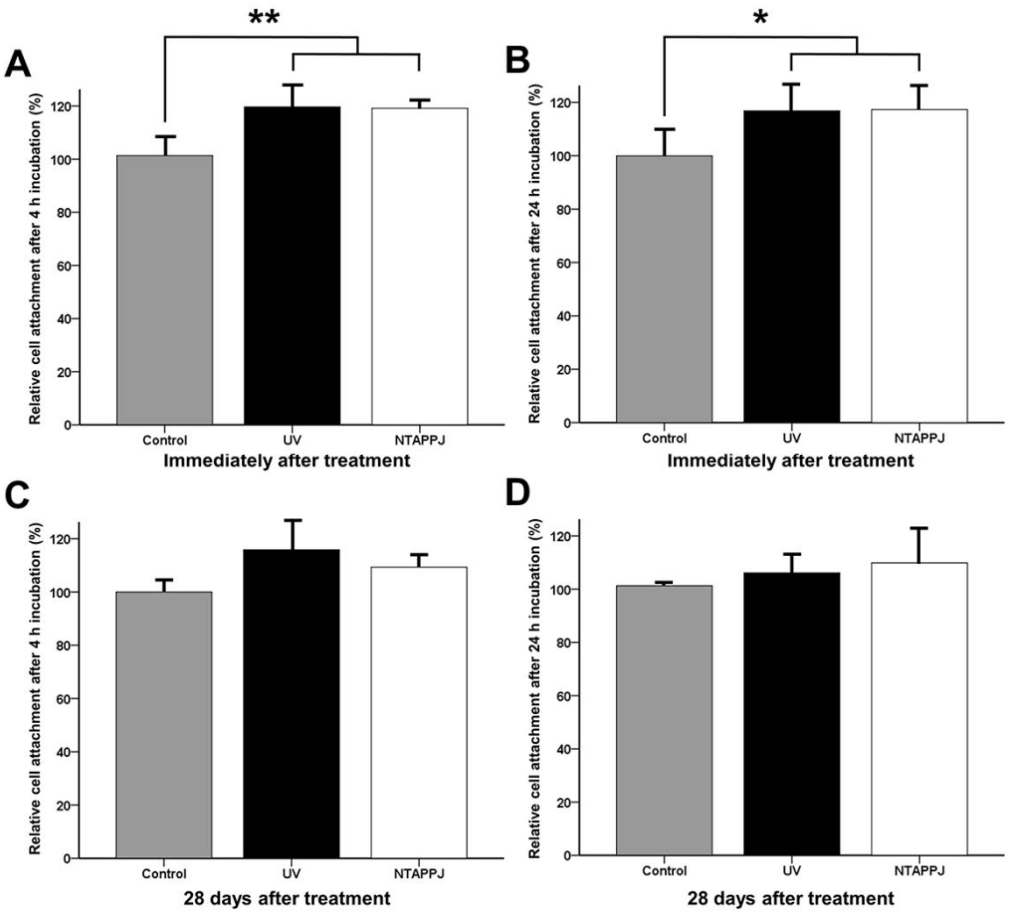

Figure 13. Changes in relative osteoblastic cell attachment rates on the titanium disc surface after treatment over time. Cell attachment rates immediately after treatment after 4 h (A) and 24 h (B) of incubation and 28 days after treatment after 4 h (C) and 24 h (D) of incubation. *$P < 0.05$, **$P < 0.01$ for comparisons between groups.

6. Changes in cellular morphology in the UV- and NTAPPJ-treated groups

After 4 h of incubation, larger osteoblastic cells with extended actin filaments and a spindle shape were observed on UV- and NTAPPJ-treated titanium discs used immediately after treatment as compared with that in the control group, which exhibited a circular shape (Figure 14B). The mean cell area, perimeter, and Feret's diameter of the osteoblastic cells on the titanium disc surface immediately after UV or NTAPPJ treatment were significantly greater than those of the control group ($P < 0.001$; Figure 14C). However, 28 days after treatment, there were no marked differences in cytomorphology between the three groups, indicating that there was a significantly delay in cellular spread and cytoskeleton development when cells were grown on the surfaces of 28-day-old treated titanium discs (Figure 14B, C).

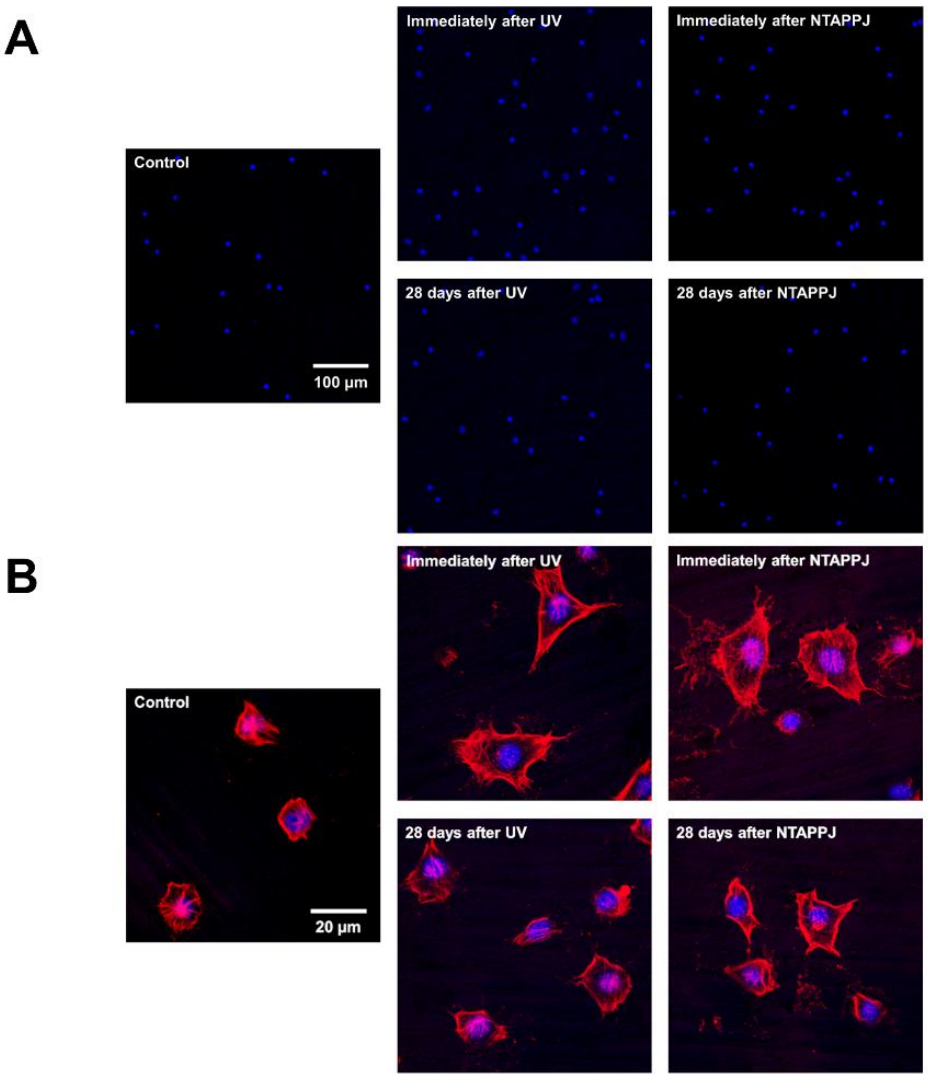

(Continued on next page)

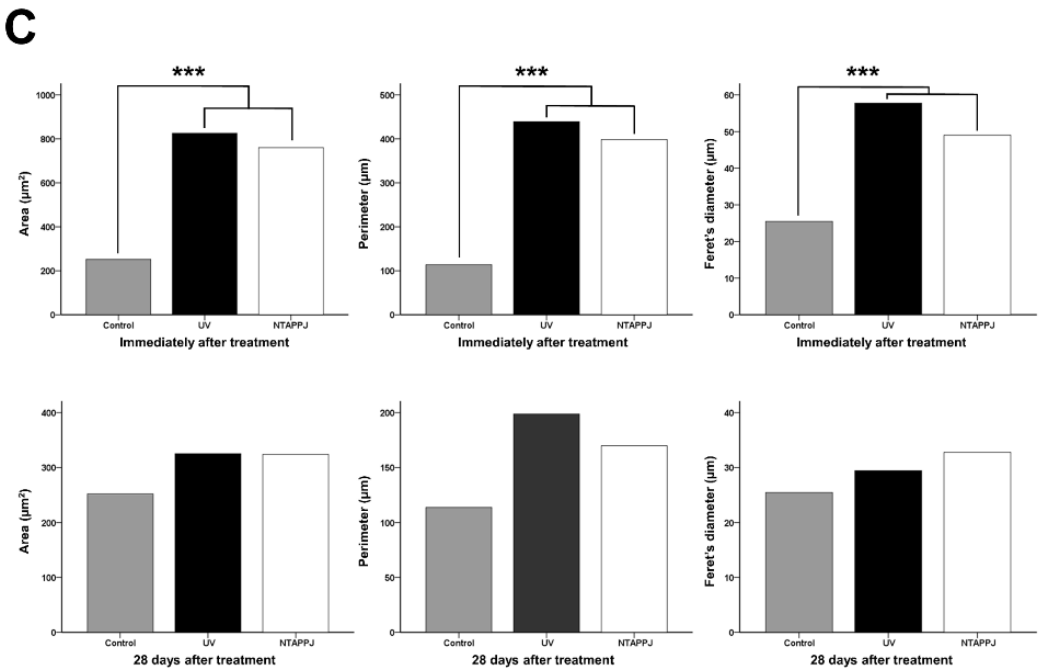

Figure 14. Changes in cellular morphology on the titanium disc surface after treatment over time. Fluorescent stained (A) blue coloration for nuclei using DAPI and (B) red coloration for F-actin filaments using rhodamine phalloidin. (C) Comparison of cytoskeleton development, including area, perimeter, and Feret's diameter of the cells, after treatment at each time point. ***$P < 0.001$ for comparisons between groups.

7. Enhanced ALP activity in UV- and NTAPPJ-treated groups

After 7 days of incubation, the ODs of UV- and NTAPPJ-treated titanium discs were slightly but significantly greater than that of the control group, regardless of the storage time (Figure 15A–C; $P = 0.015$ at immediately after treatment and $P = 0.011$ at 28 days after treatment). The ALP activity of the experimental groups was relatively constant over time, indicating that the numbers of living cells on the treated titanium disc surfaces were greater than that of the control group, regardless of the storage time, after 7 days of incubation.

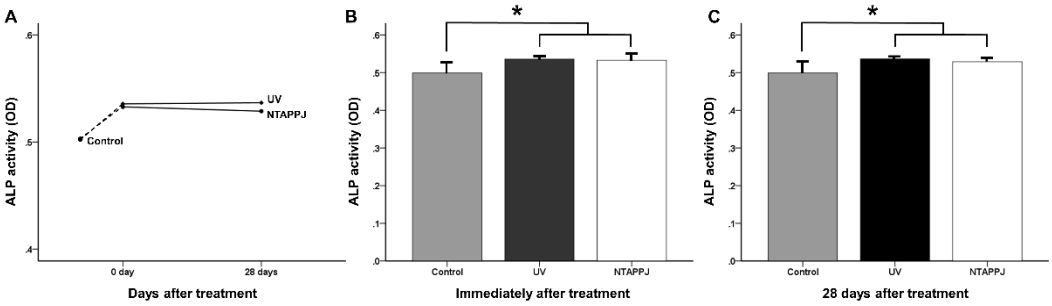

Figure 15. (A) Changes in ALP activity of the titanium disc surface after treatment over time, as determined by measuring the optical density (OD). Comparison of OD values immediately (B) and 28 days (C) after treatment between groups. *$P < 0.05$ for comparisons between groups.

IV. DISCUSSION

In this study, we aimed to evaluate time-dependent biological effects after UV and NTAPPJ treatment on aged titanium surface compared with that of untreated titanium surface. Importantly, we found that there were no differences in surface characteristics, protein adsorption, and cellular responses between UV and NTAPPJ treatments regardless of the storage time. The effects of 28-day-old treated titanium discs were not sufficient to enhance cell attachment and cytoskeleton development compared with the control group. However, ALP levels, indicating the degree of cellular differentiation, were maintained, regardless of the type of treatment and storage time. These data provide important insights into the effects of surface modifications on titanium implants for clinical applications.

The physical and reactive chemistry of NTAPPJ can be derived from the production of an electric field capable of ionising air or a carrier gas, such as nitrogen, helium, and argon, at atmospheric pressure (Bardos and Barankova, 2010; Flynn et al., 2016). From economic and clinical perspectives, it may also be desirable to utilise gases that are less expensive and easily available in the clinic, such as air, for applications involving NTAPPJ. Seo et al also reported that air-based NTAPPJ using clinical-grade compressed air for 10 min was sufficient to increase cellular responses on the titanium nanotube surface as most dental clinics have built-in air compressors (Seo et al., 2014). Based on

the above-mentioned information, this study selected air-based NTAPPJ for 10 min to treat the titanium discs.

In this study, UV and NTAPPJ treatment did not significantly alter the surface roughness parameters when analysed immediately after treatment; however, both methods increased the hydrophilicity and wettability of the titanium disc surface. Aita et al. reported that UV treatment decreases the percentage of hydrocarbons on the titanium surface without any changes to the surface roughness. Additionally, these physicochemical changes are associated with the photocatalytic phenomena of TiO_2, and the hydrocarbon level is strongly associated with the rates of protein adsorption and cell attachment (Aita et al., 2009). Similarly, NTAPPJ causes an increase in hydrophilicity and a decrease in contact angle due to the effects of removal of hydrocarbon from the titanium surface (Attri et al., 2015; Duske et al., 2012; Seo et al., 2014; Seo et al., 2015).

Nevertheless, most previous studies investigating the effects of UV and NTAPPJ on hydrophilicity did not consider the duration of the effect or the consequent rehydrophobisation (i.e. decreased hydrophilicity) of the titanium surface after such treatment, which occurs rapidly in air (Iwasa et al., 2011; Rupp et al., 2002; Rupp et al., 2014). Our results showed that the hydrophilicity of the titanium disc surface decreased rapidly within 3 days in both the UV- and NTAPPJ-treated groups, reaching half that of the control group by 28 days after treatment. Consistent with the above results, XPS showed that the peak corresponding to C1s and the atomic percentage of carbon increased over time. The increase in carbon content in the experimental groups was small; however,

its effects may have a great impact on changes in hydrophilicity and on cellular responses because the hydrophobic hydrocarbon-contaminated surface can cause entrapment of air bubbles, interfering with the interaction between proteins and cells (Rupp et al., 2014).

We found that the peak corresponding to the hydroxyl groups (-OH) of UV- and NTAPPJ-treated titanium discs were increased compared with those in the control group. During UV treatment, when removing the hydrocarbons from the TiO_2 surface, photolysis creates an electron-hole pair because of electrons in the valence band of the semiconductor, which transition to the conduction band (Hashimoto et al., 2005; Wu et al., 2015). This phenomenon causes the generation of surface oxygen vacancies, superoxide, and reactive oxygen species (ROS), such as the hydroxyl radical (Figure 16).

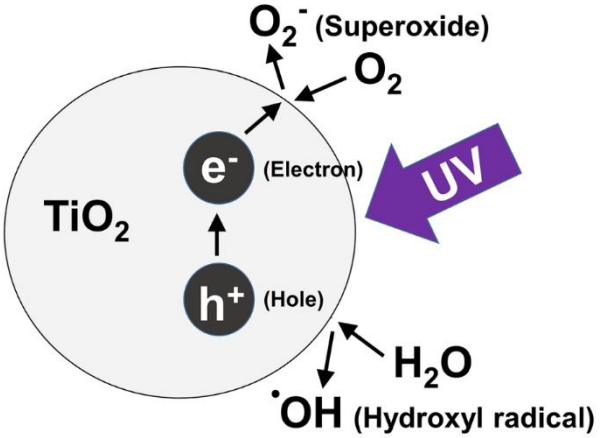

Figure 16. Photocatalytic activity by UV. The strong oxidation power of the hole enables a one-electron oxidation step with water to produce a hydroxyl radical. Oxygen can act as an electron acceptor, and be reduced by the promoted electron in the conduction band to form a superoxide ion.

In particular, NTAPPJ treatment caused an increase in ROS on the titanium surface, as measured immediately after treatment, compared with that in the UV-treated and control groups; consequently, the level of hydrophilicity and surface zeta potential of the NTAPPJ-treated titanium surface were relatively higher than those of the UV-treated titanium surface. The resulting products, such as energetic ions, UV/vacuum UV radiation, charged particles, and ROS, have broadened the scope of NTAPPJ for medical applications from sterilisation to cancer treatment (Figure 17) (Brulle et al., 2012; Kalghatgi et al., 2011; Norberg et al., 2015; Yan et al., 2016).

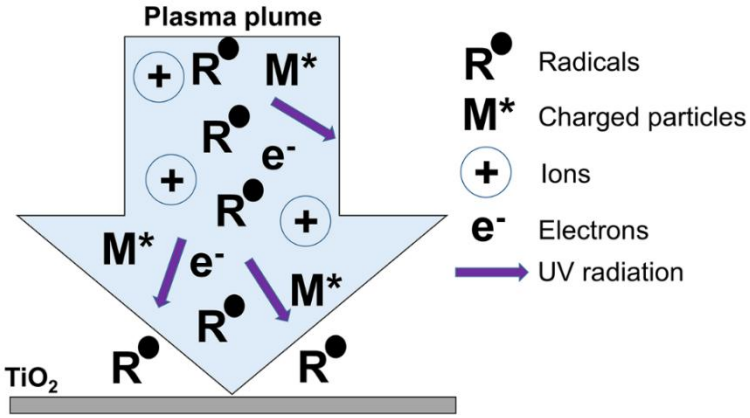

Figure 17. The plasma plume of the NTAPPJ. The resulting production of reactive radicals (reactive oxygen and nitrogen species), charged particles, ions, electrons, UV radiation have motivated the use of NTAPPJ for medical applications.

The distribution of hydroxyl radicals generated from the plasma plume is affected by the presence of a target, its nature (electrical conductivity) and humidity (dry and wet

surface), the gas flow rate, and the voltage amplitude (Darny et al., 2014; Ries et al., 2014; Yonemori and Ono, 2014). Norberg et al revealed that the electric field produced at the surface of the metal substrate is created by the accumulation of positively charged species near the surface as the electrons flow into the metal (Norberg et al., 2015).

In this study, immediately after treatment, the surface zeta potential and albumin adsorption capacity were significantly increased. In contrast, in 28-day-old treated titanium discs, these effects were decreased but were still higher than those in the control group. Untreated titanium surface that have aged for a sufficient period are known to be electronegatively charged, similar to serum albumin molecules (Att et al., 2009). After treatment using UV or NTAPPJ, the negative charge on the titanium surface decreased and consequently increased the protein adsorption rates. These chemo-attractions can enhance cell adhesion ratios because extracellular matrix protein also has a negative charge. In this study, in discs used immediately after UV or NTAPPJ treatment, the amount of cell attachment increased after 4 and 24 h of incubation. In addition, the rates of cell attachment tended to plateau after 4 h of incubation, indicating that the process of cell attachment was accelerated by these treatments. However, 28-day-old treated titanium discs did not exhibit increased cell adhesion compared with the control group. Cellular morphometry also showed that the level of cytoskeleton development on the surface of 28-day-old treated titanium discs was not significantly different between groups. However, ALP levels, indicating the degree of early cellular differentiation and

the amount of living cells on the treated titanium disc surface, were maintained, regardless of the type of treatment and storage time.

As mentioned above, these results revealed that the effects of treatment using UV or NTAPPJ on the titanium surface, which altered the negatively charged, hydrophobic (bioinert) surface to a relatively positively charged, hydrophilic (bioactive) surface, may not last to promote surrounding cell adhesion 28 days after treatment. However, this effect could still enhance osteoblast maturation after 7 days of incubation compared with that in the control group, which exhibited a hydrophobic surface.

When placing titanium implants, the first healing step is formation of a fibrin blood clot. Based on our findings, UV- or NTAPPJ-treated titanium surfaces could significantly enhance the absorption of albumin, a major plasma protein, until 4 weeks after treatment. Albumin serves as a bridging scaffold to attract mesenchymal stem cells and promote their migration through its cell-attracting terminal Arg-Gly-Asp (RGD) sequence (Att et al., 2009). The ligand-binding interaction between the RGD terminal of the adsorbed protein and integrin from the cell membrane can act as a chemoattractant (Elmengaard et al., 2005). Thus, even if the hydrophilic state of the treated titanium surface cannot be maintained for 4 weeks needed for wound healing with marked woven bone formation and maturation after implantation, this state may promote the differentiation of already attached osteoblastic cells to the bone matrix formation/maturation and mineralization stages and maintain ALP activity (Choi et al., 1996; Eriksson et al., 2004; Hoemann et al., 2009; Kawase et al., 2014; Steinbeck et al., 2013).

Titanium implant products, regardless of their applications in the medical and dental fields, are also commercially available as storage devices. Although UV and NTAPPJ can alleviate the biological aging of titanium until 4 weeks, i.e. at least the time required for initial healing, the requirement for treatment of the titanium surface for at least 10 min each time just before surgery may be challenging to surgeons in the operating room. Based on the results of our current study, pretreatment of titanium implants with UV or NTAPPJ may be applicable if appropriate storage methods are used to maintain the hydrophilicity of the titanium surface, similar to that observed immediately after treatment. Commercially, the ultimate goal is the development of treatment strategies using UV or NTAPPJ titanium implants that are not aged, regardless of the storage time.

Taken together, our findings demonstrated that UV and NTAPPJ treatment could improve the hydrophilicity of the titanium surface, contributing to enhancement and maintenance of the biological activity and interactions between blood proteins and osteoblastic cells until 4 weeks. These changes could thus increase early osseointegration between titanium implants and surrounding bone and reduce healing time, allowing patients to return to their normal lifestyles more quickly.

Several limitations to this study should be considered when interpreting these data. First, because UV is delivered to the entire titanium disc surface, NTAPPJ was focused on the titanium disc surface under jet plume, based on previous studies using the same method (Seo et al., 2014; Seo et al., 2015; Uhm et al., 2014; Yoo et al., 2015). Previous studies have reported that NTAPPJ can affect the far side of a material from the

irradiation centre owing to incorporation of air from the periphery of the jet or the admixture of a few percent with respect to the noble background gas (Lee et al., 2013; Ries et al., 2014; Uhm and Hong, 2011). Lee et al. reported that on the polystyrene plates, the range of the effects of NTAPPJ could be roughly calculated by the distance between the centre and far-side parts, at least 14.5 mm from the plume (Lee et al., 2013). However, by LIF measurements, previous studies have revealed that the density of hydroxyl radicals is highest at the centre of the plasma jet on the metal surface, but decreases gradually as the distance from the axis increases (Ries et al., 2014; Yonemori and Ono, 2014). Second, in this study, because the titanium samples were flat discs measuring 12 mm in diameter, the results from this study may not be applicable to the actual clinical setting, because the sizes of the titanium sample and the single plasma jet were too small to apply to complex prosthetic orthopaedic implants, particularly hip or knee joint prostheses in real situations. In order to facilitate processing of complex or large surfaces, other plasma sources, including multijet arrays (Robert et al., 2015), spatially extended atmospheric plasma (SEAP) arrays (Cao et al., 2010), and surface dielectric barrier discharge (DBD) plasma (Daeschlein et al., 2012), have been developed. Future studies using these sources need to determine the clinical applicability of nonthermal plasma in the treatment of complex and large orthopaedic implants. Additionally, *in vivo* experiments are necessary to confirm whether these preliminary results can be applied in real clinical situations in the medical and dental fields to ensure the long-term survival rates of the titanium implants, particularly in compromised patients.

V. CONCLUSION

Despite the limitations of this study, we found that there were no differences in the biological effects of treatment using UV or NTAPPJ on the surfaces of grade IV machined titanium discs over time. Photocatalytic activity by UV and higher production of ROS such as hydroxyl radical or synergistic ROS/UV action by NTAPPJ removed the surface hydrocarbon and altered the surface from negatively charged and hydrophobic (bioinert) to relatively positively charged and hydrophilic (bioactive), thereby enhancing protein adsorption, early pre-osteoblastic cell attachment, and cytoskeleton development. Even if this effect may not last for 28 days to promote cell adhesion and cytoskeleten development, ALP activity of the UV- and NTAPPJ-treated groups was significantly increased when compared with that of the untreated titanium. UV and NTAPPJ treatment can enhance the biological activity of aged titanium surface compared with that of untreated titanium regardless of the storage time. Future *in vivo* studies are necessary to confirm whether these results can be applied in real clinical situations in the medical and dental fields.

REFERENCES

Aita H, Hori N, Takeuchi M, Suzuki T, Yamada M, Anpo M, et al.: The effect of ultraviolet functionalization of titanium on integration with bone. *Biomaterials* 30(6): 1015-1025, 2009.

Albrektsson T, Johansson C: Osteoinduction, osteoconduction and osseointegration. *Eur Spine J* 10 Suppl 2: S96-101, 2001.

Att W, Hori N, Takeuchi M, Ouyang J, Yang Y, Anpo M, et al.: Time-dependent degradation of titanium osteoconductivity: an implication of biological aging of implant materials. *Biomaterials* 30(29): 5352-5363, 2009.

Attri P, Kim YH, Park DH, Park JH, Hong YJ, Uhm HS, et al.: Generation mechanism of hydroxyl radical species and its lifetime prediction during the plasma-initiated ultraviolet (UV) photolysis. *Sci Rep* 5: 9332, 2015.

Bacakova L, Filova E, Parizek M, Ruml T, Svorcik V: Modulation of cell adhesion, proliferation and differentiation on materials designed for body implants. *Biotechnol Adv* 29(6): 739-767, 2011.

Bardos L, Barankova H: Cold atmospheric plasma: Sources, processes, and applications. *Thin Solid Films* 518(23): 6705-6713, 2010.

Brulle L, Vandamme M, Ries D, Martel E, Robert E, Lerondel S, et al.: Effects of a non thermal plasma treatment alone or in combination with gemcitabine in a MIA PaCa2-luc orthotopic pancreatic carcinoma model. *PLoS One* 7(12): e52653, 2012.

Canullo L, Genova T, Tallarico M, Gautier G, Mussano F, Botticelli D: Plasma of Argon Affects the Earliest Biological Response of Different Implant Surfaces: An In Vitro Comparative Study. *J Dent Res* 95(5): 566-573, 2016.

Cao Z, Nie Q, Bayliss DL, Walsh JL, Ren CS, Wang DZ, et al.: Spatially extended atmospheric plasma arrays. *Plasma Sources Sci Technol* 19(2), 2010.

Choi JY, Lee BH, Song KB, Park RW, Kim IS, Sohn KY, et al.: Expression patterns of bone-related proteins during osteoblastic differentiation in MC3T3-E1 cells. *J Cell Biochem* 61(4): 609-618, 1996.

Choi SH, Jang SH, Cha JY, Hwang CJ: Evaluation of the surface characteristics of anodic oxidized miniscrews and their impact on biomechanical stability: An experimental study in beagle dogs. *Am J Orthod Dentofacial Orthop* 149(1): 31-38, 2016.

Daeschlein G, Scholz S, Arnold A, von Podewils S, Haase H, Emmert S, et al.: In Vitro Susceptibility of Important Skin and Wound Pathogens Against Low Temperature Atmospheric Pressure Plasma Jet (APPJ) and Dielectric Barrier Discharge Plasma (DBD). *Plasma Process Polym* 9(4): 380-389, 2012.

Dalago HR, Schuldt Filho G, Rodrigues MA, Renvert S, Bianchini MA: Risk indicators for Peri-implantitis. A cross-sectional study with 916 implants. *Clin Oral Implants Res*, 2016.

Darny T, Robert E, Ries D, Dozias S, Pouvesle JM: Unexpected Plasma Plume Shapes Produced by a Microsecond Plasma Gun Discharge. *IEEE Trans Plasma Sci IEEE Nucl Plasma Sci Soc* 42(10): 2504-2505, 2014.

Degidi M, Piattelli A, Shibli JA, Perrotti V, Iezzi G: Bone Formation Around Immediately Loaded and Submerged Dental Implants with a Modified Sandblasted and Acid-Etched Surface After 4 and 8 Weeks: A Human Histologic and Histomorphometric Analysis. *Int J Oral Maxillofac Implants* 24(5): 896-900, 2009.

Drees P, Eckardt A, Gay RE, Gay S, Huber LC: Mechanisms of Disease: molecular insights into aseptic loosening of orthopedic implants. *Nat Clin Pract Rheumatol* 3(3): 165-171, 2007.

Duske K, Koban I, Kindel E, Schroder K, Nebe B, Holtfreter B, et al.: Atmospheric plasma enhances wettability and cell spreading on dental implant metals. *J Clin Periodontol* 39(4): 400-407, 2012.

Elmengaard B, Bechtold JE, Soballe K: In vivo study of the effect of RGD treatment on bone ongrowth on press-fit titanium alloy implants. *Biomaterials* 26(17): 3521-3526, 2005.

Eriksson C, Nygren H, Ohlson K: Implantation of hydrophilic and hydrophobic titanium discs in rat tibia: cellular reactions on the surfaces during the first 3 weeks in bone. *Biomaterials* 25(19): 4759-4766, 2004.

Fender D, Harper WM, Gregg PJ: The trent regional arthroplasty study - Experiences with a hip register. *J Bone Joint Surg Br* 82B(7): 944-947, 2000.

Flynn PB, Busetti A, Wielogorska E, Chevallier OP, Elliott CT, Laverty G, et al.: Non-thermal Plasma Exposure Rapidly Attenuates Bacterial AHL-Dependent Quorum Sensing and Virulence. *Sci Rep* 6: 26320, 2016.

Fransson C, Wennstrom J, Berglundh T: Clinical characteristics at implants with a history of progressive bone loss. *Clin Oral Implants Res* 19(2): 142-147, 2008.

Gapski R, Wang HL, Mascarenhas P, Lang NP: Critical review of immediate implant loading. *Clin Oral Implants Res* 14(5): 515-527, 2003.

Giro G, Tovar N, Witek L, Marin C, Silva NR, Bonfante EA, et al.: Osseointegration assessment of chairside argon-based nonthermal plasma-treated Ca-P coated dental implants. *J Biomed Mater Res A* 101(1): 98-103, 2013.

Hashimoto K, Irie H, Fujishima A: TiO2 photocatalysis: A historical overview and future prospects. *Jpn J Appl Phys Pt 1* 44(12): 8269-8285, 2005.

Hayashi M, Jimbo R, Xue Y, Mustafa K, Andersson M, Wennerberg A: Photocatalytically induced hydrophilicity influences bone remodelling at longer healing periods: a rabbit study. *Clin Oral Implants Res* 25(6): 749-754, 2014.

Hirakawa Y, Jimbo R, Shibata Y, Watanabe I, Wennerberg A, Sawase T: Accelerated bone formation on photo-induced hydrophilic titanium implants: an experimental study in the dog mandible. *Clin Oral Implants Res* 24 Suppl A100: 139-144, 2013.

Hoemann CD, El-Gabalawy H, McKee MD: In vitro osteogenesis assays: influence of the primary cell source on alkaline phosphatase activity and mineralization. *Pathol Biol (Paris)* 57(4): 318-323, 2009.

Hong YC, Kang WS, Hong YB, Yi WJ, Uhm HS: Atmospheric pressure air-plasma jet evolved from microdischarges: Eradication of E. coli with the jet. *Phys Plasmas* 16(12), 2009.

Iwasa F, Tsukimura N, Sugita Y, Kanuru RK, Kubo K, Hasnain H, et al.: TiO2 micro-nano-hybrid surface to alleviate biological aging of UV-photofunctionalized titanium. *Int J Nanomedicine* 6: 1327-1341, 2011.

Kalghatgi S, Kelly CM, Cerchar E, Torabi B, Alekseev O, Fridman A, et al.: Effects of non-thermal plasma on mammalian cells. *PLoS One* 6(1): e16270, 2011.

Kawase T, Tanaka T, Minbu H, Kamiya M, Oda M, Hara T: An atmospheric-pressure plasma-treated titanium surface potentially supports initial cell adhesion, growth, and

differentiation of cultured human prenatal-derived osteoblastic cells. *J Biomed Mater Res B Appl Biomater* 102(6): 1289-1296, 2014.

Kim HM, Himeno T, Kawashita M, Lee JH, Kokubo T, Nakamura T: Surface potential change in bioactive titanium metal during the process of apatite formation in simulated body fluid. *J Biomed Mater Res A* 67(4): 1305-1309, 2003.

Le Guehennec L, Soueidan A, Layrolle P, Amouriq Y: Surface treatments of titanium dental implants for rapid osseointegration. *Dent Mater* 23(7): 844-854, 2007.

Lee JH, Kwon JS, Kim YH, Choi EH, Kim KM, Kim KN: The effects of enhancing the surface energy of a polystyrene plate by air atmospheric pressure plasma jet on early attachment of fibroblast under moving incubation. *Thin Solid Films* 547: 99-105, 2013.

Lee JH, Ogawa T: The biological aging of titanium implants. *Implant Dent* 21(5): 415-421, 2012.

Minamikawa H, Ikeda T, Att W, Hagiwara Y, Hirota M, Tabuchi M, et al.: Photofunctionalization increases the bioactivity and osteoconductivity of the titanium alloy Ti6Al4V. *J Biomed Mater Res A* 102(10): 3618-3630, 2014.

Misch CE, Dietsh-Misch F, Hoar J, Beck G, Hazen R, Misch CM: A bone quality-based implant system: first year of prosthetic loading. *J Oral Implantol* 25(3): 185-197, 1999.

Norberg SA, Johnsen E, Kushner MJ: Helium atmospheric pressure plasma jets touching dielectric and metal surfaces. *J Appl Phys* 118(1), 2015.

Pyo SW, Park YB, Moon HS, Lee JH, Ogawa T: Photofunctionalization enhances bone-implant contact, dynamics of interfacial osteogenesis, marginal bone seal, and removal torque value of implants: a dog jawbone study. *Implant Dent* 22(6): 666-675, 2013.

Rani VV, Vinoth-Kumar L, Anitha VC, Manzoor K, Deepthy M, Shantikumar VN: Osteointegration of titanium implant is sensitive to specific nanostructure morphology. *Acta Biomater* 8(5): 1976-1989, 2012.

Ries D, Dilecce G, Robert E, Ambrico PF, Dozias S, Pouvesle JM: LIF and fast imaging plasma jet characterization relevant for NTP biomedical applications. *Journal of Physics D-Applied Physics* 47(27), 2014.

Robert E, Darny T, Dozias S, Iseni S, Pouvesle JM: New insights on the propagation of pulsed atmospheric plasma streams: From single jet to multi jet arrays. *Phys Plasmas* 22(12), 2015.

Rupp F, Axmann D, Ziegler C, Geis-Gerstorfer J: Adsorption/desorption phenomena on pure and Teflon AF-coated titania surfaces studied by dynamic contact angle analysis. *J Biomed Mater Res* 62(4): 567-578, 2002.

Rupp F, Gittens RA, Scheideler L, Marmur A, Boyan BD, Schwartz Z, et al.: A review on the wettability of dental implant surfaces I: theoretical and experimental aspects. *Acta Biomater* 10(7): 2894-2906, 2014.

Seo HY, Kwon JS, Choi YR, Kim KM, Choi EH, Kim KN: Cellular attachment and differentiation on titania nanotubes exposed to air- or nitrogen-based non-thermal atmospheric pressure plasma. *PLoS One* 9(11): e113477, 2014.

Seo SH, Uhm SH, Kwon JS, Choi EH, Kim KM, Kim KN: An Alternative to Annealing TiO2 Nanotubes for Morphology Preservation: Atmospheric Pressure Plasma Jet Treatment. *J Nanosci Nanotechnol* 15(3): 2501-2507, 2015.

Shen J, Liu J, Chen X, Wang X, He F, Wang H: The In Vivo Bone Response of Ultraviolet-Irradiated Titanium Implants Modified with Spontaneously Formed Nanostructures: An Experimental Study in Rabbits. *Int J Oral Maxillofac Implants* 31(4): 776-784, 2016.

Simonis P, Dufour T, Tenenbaum H: Long-term implant survival and success: a 10-16-year follow-up of non-submerged dental implants. *Clin Oral Implants Res* 21(7): 772-777, 2010.

Steinbeck MJ, Chernets N, Zhang J, Kurpad DS, Fridman G, Fridman A, et al.: Skeletal Cell Differentiation Is Enhanced by Atmospheric Dielectric Barrier Discharge Plasma Treatment. *PLoS One* 8(12), 2013.

Teixeira HS, Marin C, Witek L, Freitas A, Jr., Silva NR, Lilin T, et al.: Assessment of a chair-side argon-based non-thermal plasma treatment on the surface characteristics and integration of dental implants with textured surfaces. *J Mech Behav Biomed Mater* 9: 45-49, 2012.

Tuna T, Wein M, Swain M, Fischer J, Att W: Influence of ultraviolet photofunctionalization on the surface characteristics of zirconia-based dental implant materials. *Dent Mater* 31(2): e14-24, 2015.

Uchiyama H, Yamada M, Ishizaki K, Sakurai K: Specific ultraviolet-C irradiation energy for functionalization of titanium surface to increase osteoblastic cellular attachment. *J Biomater Appl* 28(9): 1419-1429, 2014.

Uhm HS, Hong YC: Various microplasma jets and their sterilization of microbes. *Thin Solid Films* 519(20): 6974-6980, 2011.

Uhm SH, Song DH, Kwon JS, Lee SB, Han JG, Kim KN: Tailoring of antibacterial Ag nanostructures on TiO2 nanotube layers by magnetron sputtering. *J Biomed Mater Res B Appl Biomater* 102(3): 592-603, 2014.

Wang R, Hashimoto K, Fujishima A, Chikuni M, Kojima E, Kitamura A, et al.: Light-induced amphiphilic surfaces. *Nature* 388(6641): 431-432, 1997.

Wennerberg A, Svanborg LM, Berner S, Andersson M: Spontaneously formed nanostructures on titanium surfaces. *Clin Oral Implants Res* 24(2): 203-209, 2013.

Wu JY, Zhou L, Ding XL, Gao Y, Liu XN: Biological Effect of Ultraviolet Photocatalysis on Nanoscale Titanium with a Focus on Physicochemical Mechanism. *Langmuir* 31(36): 10037-10046, 2015.

Yan D, Nourmohammadi N, Bian K, Murad F, Sherman JH, Keidar M: Stabilizing the cold plasma-stimulated medium by regulating medium's composition. *Sci Rep* 6: 26016, 2016.

Yonemori S, Ono R: Flux of OH and O radicals onto a surface by an atmospheric-pressure helium plasma jet measured by laser-induced fluorescence. *Journal of Physics D-Applied Physics* 47(12), 2014.

Yoo EM, Uhm SH, Kwon JS, Choi HS, Choi EH, Kim KM, et al.: The Study on Inhibition of Planktonic Bacterial Growth by Non-Thermal Atmospheric Pressure Plasma Jet Treated Surfaces for Dental Application. *J Biomed Nanotechnol* 11(2): 334-341, 2015.

Abstract (Korean)

자외선 및 저온 대기압 플라즈마 처리 후 시간에 따른 타이타늄의 생물학적 활성도 변화

최 성 환

연세대학교 대학원 치의학과

(지도교수 : 황 충 주)

자외선 (UV) 또는 저온 대기압 플라즈마 (NTAPPJ) 처리는 타이타늄 임플란트 표면의 형태적인 변화없이 물리 화학적 특성을 변화시키고, 혈장 단백질 및 골모 세포의 부착을 촉진시켜 새로운 골의 형성을 증가시키는 것과 같은 타이타늄의 생물학적 활성도를 향상 시키는 것으로 알려져 왔다. 그러나, UV 와 NTAPPJ 간에 처리 후 시간에 따른 타이타늄 표면의 생물학적 활성도의

차이 여부를 평가한 연구는 거의 없었다. 따라서 본 연구는 UV 와 NTAPPJ 처리 후 시간에 따른 타이타늄의 생물학적 활성도의 변화를 아무런 처리하지 않은 타이타늄과 비교하여 평가하였다.

지름 12 mm 의 평활면 grade IV 타이타늄 디스크에 UV 를 15 분간 또는 NTAPPJ 를 10 분간 처리한 후 즉시 또는 28 일 동안 보관한 뒤 시편으로 사용하였다. 시간에 따른 타이타늄 표면의 특성 변화를 평가하기 위해서 주사 전자 현미경, 표면 조도계, 접촉각 측정기, 광전자 분광기, 제타 전위 측정기를 이용하였다. 타이타늄의 시간에 따른 생물학적 활성도의 변화를 평가하기 위해서 소 혈청 알부민 부착률, 백서 골모 유사 세포인 MC3T3-E1 의 초기 부착률, 세포 골격 발달 수준 및 알카라인 포스파타제 (ALP)의 활성도를 분석하였다.

UV 와 NTAPPJ 가 타이타늄 표면에 미치는 효과는 보관 기간에 상관없이 서로 간에 유의한 차이를 보이지 않았다 ($P > 0.05$). UV 에 의한 광촉매 현상과 NTAPPJ 에 의한 하이드록실 라디칼과 같은 활성 산소종 (ROS)의 증가 또는 ROS/UV 의 상승 효과는 표면의 탄화 수소를 제거하였고, 표면을 음극의 소수성 (생체 불활성)에서 양극의 친수성 (생체 활성)으로 변화시켰다 ($P < 0.001$). 이들 처리 직후에는 알부민 부착률 ($P < 0.001$)과 골모 세포의 초기 부착률이 증가하였고 ($P < 0.05$), 세포 골격 또한 더욱 발달하였다 ($P < 0.001$).

UV 와 NTAPPJ 처리 28 일 후, 세포 부착률과 세포 골격의 발달 수준은 그룹 간에 유의한 차이를 보이지 않았다 ($P > 0.05$). 그러나, UV 와 NTAPPJ 처리한 군의 ALP 활성도는 아무런 처리하지 않은 타이타늄과 비교하였을 때 유의하게 증가하였다 ($P < 0.05$).

본 연구의 결과를 토대로, UV 와 NTAPPJ 가 타이타늄 표면에 미치는 생물학적 효과는 시간에 상관없이 서로 간에 유의한 차이를 보이지 않았다. 처리 직후와 비교하였을 때, 이들 처리 효과는 시간이 지날수록 감소하였다. 그러나 UV 와 NTAPPJ 처리는 보관 기간에 상관없이 노화된 타이타늄 표면의 생물학적 활성도를 아무런 처리하지 않은 타이타늄에 비해 증가시킬 수 있을 것이다. 향후 이러한 결과가 의학 및 치의학 분야의 실제 임상에서 적용될 수 있는지 여부를 확인하기 위해 *in vivo* 연구가 필요하다고 생각된다.

핵심되는 말 : 타이타늄; 임플란트; 자외선; 저온 대기압 플라즈마; 친수성; 탄화수소; 광촉매 현상; 활성 산소종; 생물학적 활성도